Applied Mathematics and Computation 216 (2010) 3265–3274

Contents lists available at ScienceDirect

Applied Mathematics and Computation

journal homepage: www.elsevier.com/locate/amc

Parameter extension for combined hybrid finite element methods and application to plate bending problems ☆

Guozhu Yu [a], Xiaoping Xie [a,*], Xu Zhang [b]

[a] School of Mathematics, Sichuan University, Chengdu 610064, China
[b] Department of Mathematics, Virginia Tech, Blacksburg, VA 24061, USA

ARTICLE INFO

Keywords:
Finite element method
Hybrid element
Plate bending
Adini's element
Galerkin/least-squares

ABSTRACT

Based on a weighted average of the modified Hellinger–Reissner principle and its dual, the combined hybrid finite element (CHFE) method was originally proposed with a combination parameter limited in the interval $(0,1)$. In actual computation this parameter plays an important role in adjusting the energy error of discretization models. In this paper, a novel expression of the combined hybrid variational form is used to show the relationship between the resultant method and some Galerkin/least-squares stabilized finite scheme for plate bending problems. The choice of combination parameter is then extended to $(-\infty,0)\bigcup(0,1)$. Existence, uniqueness and convergence of the solution of discrete schemes are proved, and the advantage of the parameter extension in computation is discussed. As an application, improvement of Adini's rectangular element by the CHFE approach is performed.

1. Introduction

The combined hybrid finite element (CHFE) method is a special stabilized mixed method developed in recent years for elasticity problems [1–3]. Based on a weighted average of the formulations of Hellinger–Reissner principle and its dual, the primal hybrid variational principle, this method does not require finite element pairs of stress and displacement spaces to satisfy the inf-sup or LBB conditions, and, for any given combination parameter $\alpha\in(0,1)$, it always yields a convergent numerical solution.

For fourth-order plate bending problems, due to the C^1-continuity requirement, determination of suitable displacement shape functions is much more complex than those needed for C^0-continuity. This C^1 difficulty has resulted in many mixed approaches such as hybrid formulations and least-squares methods which include the use of Lagrangian multiplier and penalty strategies (see the papers [4–18] and the references therein for details). Because of the 'saddle-point' nature of the hybrid methods, the displacement and bending moments approximations are required to satisfy the inf-sup stability condition (see, e.g. [4,6]). In [19] the CHFE approach was extended to the numerical analysis of the plate bending problems to avoid the inf-sup difficulty and to yield stabilized hybrid schemes in the sense that the displacement and bending moments variables are approximated independently.

Due to elimination of the stress/moments parameters at the element level, the CHFE method preserves the convenience of the standard Galerkin displacement scheme. Moreover, this method is shown to be of an energy-error-adjusting mechanism

☆ This work was supported in part by the Natural Science Foundation of China (10771150), the National Basic Research Program of China (2005CB321701), and the Program for New Century Excellent Talents in University (NCET-07-0584).

* Corresponding author.
E-mail addresses: yuguozhumail@yahoo.com.cn (G. Yu), xpxie@scu.edu.cn, xpxie@gmail.com (X. Xie), xuz@vt.edu (X. Zhang).

0096-3003/$ - see front matter © 2010 Elsevier Inc. All rights reserved.
doi:10.1016/j.amc.2010.04.052

[20–22], i.e. for given displacement and stress/moments modes, by changing the combination parameter α in the interval $(0,1)$ one can adjust the energy of the discretization model so as to reduce the energy error. In [20–22], it was shown numerically that the smaller the energy error is, the better the accuracy of the scheme will be. However, in some applications there are circumstances that the energy error of a CHFE scheme with a special displacement approximation can not be reduced for the parameter $\alpha \in (0,1)$ [21], so it is impossible to attain higher numerical accuracy at coarse meshes for the corresponding CHFE scheme by choosing an appropriate α in $(0,1)$. Hence, a further study of the energy-error-adjusting mechanism of the CHFE method seems to be required.

In this paper, a new survey of the CHFE method is carried out for plate bending problems so as to disclose some new interesting aspects of the method. By using a novel equivalent expression, the CHFE scheme is shown to enjoy the form of some Galerkin/least-squares stabilized finite element method [23,24]. This observation then leads to an extension of the combination parameter interval from $(0,1)$ to $(-\infty,0)\bigcup(0,1)$. As an application, improvement of Adini's plate element by the CHFE method is investigated.

Throughout the paper the letter C represents a positive constant which is independent of the mesh size $h = \max_{\Omega_i}\{h_i\}$ and may be different at its each occurrence.

2. Combined hybrid variational principle

Considering the following plate bending problem:

$$\begin{cases} \mathbf{divdiv}\sigma = f & \text{in } \Omega, \\ \sigma = \mathbf{m}(\mathbf{D}_2 u) & \text{in } \Omega, \\ u = \nabla u\cdot\mathbf{n} = 0 & \text{on } \partial\Omega, \end{cases} \tag{2.1}$$

where $\Omega \subset \Re^2$ is a bounded open set, u represents the vertical deflection, $\sigma = (\sigma_{ij})$ $(i,j = 1,2)$ denotes the symmetric bending moment tensor (i.e. $\sigma_{12} = \sigma_{21}$), $\mathbf{divdiv}\sigma = \partial_{11}\sigma_{11} + 2\partial_{12}\sigma_{12} + \partial_{22}\sigma_{22}$ with $\partial_{ij} = \frac{\partial^2}{\partial x_i \partial x_j}$ $(i,j = 1,2)$,

$$\mathbf{D}_2 u = \begin{pmatrix} \partial_{11}u & \partial_{12}u \\ \partial_{12}u & \partial_{22}u \end{pmatrix}, \quad \mathbf{m}(\sigma) = \begin{pmatrix} \sigma_{11} + \nu\sigma_{22} & (1-\nu)\sigma_{12} \\ (1-\nu)\sigma_{12} & \nu\sigma_{11} + \sigma_{22} \end{pmatrix}$$

with $\nu \in (0, 0.5)$ the Poisson's coefficient, and $\mathbf{n}$ is the unit outer normal vector along $\partial\Omega$.

The combined hybrid variational principle corresponding to the problem (2.1) reads as [19]:

$$\inf_{(v,v_c)\in U\times U_c} \sup_{\tau\in\mathbf{V}} \left\{ \frac{1-\alpha}{2} d(v,v) - f(v) - b_1(\tau, v - v_c) + \alpha\left[b_2(\tau, v) - \frac{1}{2}a(\tau,\tau)\right]\right\}, \tag{2.2}$$

where $T_h = \{\Omega_i\}$ denotes a subdivision of Ω, h_i the diameter of Ω_i, and

$$\mathbf{V} = \prod_{\Omega_i\in T_h} H(\mathbf{divdiv}, \Omega_i) = \prod_{\Omega_i\in T_h}\left\{\tau \in \left(L^2(\Omega_i)\right)_s^4; \mathbf{divdiv}\tau \in L^2(\Omega_i)\right\},$$

$$U = \left\{ v \in \prod_{\Omega_i\in T_h} H^2(\Omega_i);\ v = \nabla v\cdot\mathbf{n} = 0,\ \mathit{on}\ \partial\Omega\right\},$$

$$U_c = H_0^2(\Omega)/\prod_{\Omega_i\in T_h} H_0^2(\Omega_i) = \left\{ \mathit{trace\ of}\ \ v \in H_0^2(\Omega)\ \mathit{on\ boundaries} \prod_{\Omega_i\in T_h}\partial\Omega_i\right\}$$

are respectively the symmetric bending moment vector space, the deflection space, and the interelemental boundary deflection space, $\left(L^2(\Omega_i)\right)_s^4$ the space of square integrable 2×2 symmetric tensors, and

$$a(\sigma,\tau) = \int_\Omega \mathbf{m}^{-1}(\sigma) : \tau\, d\mathbf{x},$$

$$b_1(\tau, v - v_c) = \sum \oint_{\partial\Omega_i} [M_{nn}(\tau)\nabla(v - v_c)\cdot\mathbf{n} + M_{ns}(\tau)\nabla(v - v_c)\cdot\mathbf{s} - Q_n(\tau)(v - v_c)]ds,$$

$$b_2(\tau, v) = \sum\int_{\Omega_i} \tau : \mathbf{D}_2 v\, d\mathbf{x},$$

$$d(u, v) = \sum\int_{\Omega_i} \mathbf{m}(\mathbf{D}_2 u) : \mathbf{D}_2 v\, d\mathbf{x},$$

$$f(v) = \int_\Omega f v\, d\mathbf{x},$$

$$M_{nn}(\tau) = (\tau\mathbf{n})\cdot\mathbf{n}, \quad M_{ns}(\tau) = (\tau\mathbf{n})\cdot\mathbf{s}, \quad Q_n(\tau) = \nabla(tr(\tau))\cdot\mathbf{n},$$

$\mathbf{n}$ = unit outer normal vector along $\partial\Omega_i$,

$\mathbf{s}$ = unit tangent vector along $\partial\Omega_i$.

According to optimality conditions of saddle-point problems, the combined hybrid variational principle (2.2) is equivalent to:

Find $(\sigma, u, u_c) \in \mathbf{V} \times U \times U_c$ such that

$$\alpha a(\sigma,\tau) - \alpha b_2(\tau,u) + b_1(\tau,u-u_c) = 0 \quad \forall \tau \in \mathbf{V}, \tag{2.3}$$

$$\alpha b_2(\sigma,v) - b_1(\sigma,v-v_c) + (1-\alpha)d(u,v) = f(v) \quad \forall (v,v_c) \in U \times U_c. \tag{2.4}$$

Let $U^h \subset U$ and $\mathbf{V}^h \subset \mathbf{V}$ be finite-dimensional subspaces equipped with norms

$$\|v\|_U = \left[\sum \int_{\Omega_i} \mathbf{m}(\mathbf{D}_2 v) : \mathbf{D}_2 v \, d\mathbf{x}\right]^{\frac{1}{2}},$$

$$\|\tau\|_{\mathbf{V}} = \left[\int_\Omega \mathbf{m}^{-1}(\tau) : \tau \, d\mathbf{x} + \sum h_i^4 |\mathbf{divdiv}\tau|^2_{0,\Omega_i}\right]^{\frac{1}{2}}.$$

To discuss finite element discretizations of problem (2.2) or its equivalent problem (2.3)–(2.4), the weakly compatible finite-dimensional deflection subspace $U^h \subset U$ is introduced [19]:

Definition 2.1. A non-conforming space U^h is weakly compatible if for $\Omega_i \in T_h$, there exists a set S_i of continuity node points on $\partial\Omega_i$, such that

(1) $d(v,v) = 0$ implies $v = 0$.
(2) An interpolation operator $T_c(v): U^h \to U_c$, i.e. the conforming component of v, can be constructed by using the set $\bigcup_{\Omega_i \in T_h} v(S_i)$ of node point values of v.

As pointed out in [19], all the conventional plate elements with C^1-continuous vertices are weakly compatible. In fact, the weakly compatible subspace U^h is of either one of the following two characteristics:

(i) The set of nodal parameters of $v \in U^h$ on each side e of element Ω_i (a triangle or a quadrilateral) is

$$\Pi_e(v) = \{v(Q_j), \partial_1 v(Q_j), \partial_2 v(Q_j), \quad j = 1,2\},$$

where Q_1 and Q_2 are the endpoints of e. And then T_c can be constructed as

$$\forall v \in U^h, \quad T_c(v)|_e \in P_3(e), \quad \nabla T_c(v) \cdot \mathbf{n}|_e \in P_1(e),$$

such that for $j = 1,2$,

$$T_c(v)(Q_j) = v(Q_j), \quad \nabla T_c(v)(Q_j) \cdot \mathbf{s} = \nabla v(Q_j) \cdot \mathbf{s},$$
$$\nabla T_c(v)(Q_j) \cdot \mathbf{n} = \nabla v(Q_j) \cdot \mathbf{n},$$

where $P_t(\Omega_i)$ denotes the set of polynomials of degree $\leqslant t$ for an integer $t \geqslant 0$;

(ii) The set of nodal parameters of $v \in U^h$ on each side e of element Ω_i is

$$\Sigma_e(v) = \{v(Q_j), \partial_1 v(Q_j), \partial_2 v(Q_j), \quad j = 1,2; \nabla v(Q_3) \cdot \mathbf{n}\},$$

where $Q_3 = Q_{12}$ is the midpoint of e. Then T_c can be constructed as

$$\forall v \in U^h, \quad T_c(v)|_e \in P_3(e), \quad \nabla T_c(v) \cdot \mathbf{n}|_e \in P_2(e),$$

such that for $j = 1,2$,

$$T_c(v)(Q_j) = v(Q_j), \quad \nabla T_c(v)(Q_j) \cdot \mathbf{s} = \nabla v(Q_j) \cdot \mathbf{s},$$

and for $j = 1,2,3$,

$$\nabla T_c(v)(Q_j) \cdot \mathbf{n} = \nabla v(Q_j) \cdot \mathbf{n}.$$

Let $\mathbf{V}^h \subset \mathbf{V}$ be a finite-dimensional subspace of piecewise-independent bending moment approximation. By virtue of the interpolation operator T_c, we take $U_c^h = T_c(U^h)$ as the approximation of the interelemental boundary deflection subspace U_c. Then the problem (2.3)–(2.4) is discretized as:

Find $(\sigma_h, u_h) \in \mathbf{V}^h \times U^h$, such that

$$\alpha a(\sigma_h,\tau) - \alpha b_2(\tau,u_h) + b_1(\tau,u_h - T_c(u_h)) = 0 \quad \forall \tau \in \mathbf{V}^h, \tag{2.5}$$

$$\alpha b_2(\sigma_h,v) - b_1(\sigma_h,v - T_c(v)) + (1-\alpha)d(u_h,v) = f(v) \quad \forall v \in U^h. \tag{2.6}$$

Remark 2.1. If the weakly compatible space $U^h \subset C^0(\bar{\Omega})$, then by the construction of T_c one has $T_c(v)|_{\partial\Omega_i} = v|_{\partial\Omega_i}$, and the following relation holds:

$$b_1(\tau, v - T_c(v)) = \sum \oint_{\partial\Omega_i} M_{nn}(\tau)\nabla(v - T_c(v)) \cdot \mathbf{n}\, ds, \quad \forall(\tau, v) \in \mathbf{V}^h \times U^h.$$

Moreover, if $U^h \subset C^1(\bar{\Omega})$, then

$$b_1(\tau, v - T_c(v)) = 0, \quad \forall(\tau, v) \in \mathbf{V}^h \times U^h.$$

Remark 2.2. Since $\tau \in \mathbf{V}^h$ is piecewise-independent, the parameters of bending moments can be eliminated at an element level.

Remark 2.3. In the case $\alpha = 0$, the combined hybrid scheme (2.5)–(2.6) is of approximate amount to the conforming or nonconforming scheme.

Remark 2.4. In the extreme case $\alpha = 1$, (2.5)–(2.6) reduces to a usual hybrid scheme, and the following inf-sup condition

$$\sup_{\tau \in \mathbf{V}^h} \frac{b_2(\tau, v) - b_1(\tau, v - T_c(v))}{\|\tau\|_{\mathbf{V}}} \geqslant C\|v\|_U, \quad \forall v \in U^h$$

is required for subspaces $\mathbf{V}^h$ and U^h to ensure the element stiffness matrix having sufficient rank.

For the combined hybrid scheme (2.5)–(2.6), it is not necessary to impose any inf-sup condition on finite element subspaces $\mathbf{V}^h \times U^h$. In fact, it holds the following convergence theorem [19]:

Lemma 2.1. *Assume that (σ, u) is the exact solution to the problem (2.1). Then for any $\alpha \in (0,1)$, there exists a unique combined hybrid finite element solution $(\sigma_h, u_h) \in \mathbf{V}^h \times U^h$ to the problem (2.5)–(2.6) and a positive constant C such that*

$$\|\sigma - \sigma_h\|_{0,\Omega} + \|u - u_h\|_U \leqslant C\left\{\inf_{\tau \in \mathbf{V}^h} \|\sigma - \tau\|_{\mathbf{V}} + \inf_{v \in U^h}\left[\|u - v\|_U + \sup_{\tau \in \mathbf{V}^h} \frac{b_1(\tau, v - T_c(v))}{\|\tau\|_{\mathbf{V}}}\right]\right\}.$$

This lemma shows that when the deflection approximation subspace U^h is given, the combined hybrid scheme (2.5)–(2.6) will give convergent finite element solutions with any bending moment mode $\mathbf{V}^h$ and any given combination parameter $\alpha \in (0,1)$. This guarantees the reliability of the CHFE method with graduate convergence at finer meshes.

In next section, the extension of the combination parameter α and its role in the energy adjustment will be discussed.

3. Combination parameter extension and energy adjustment

3.1. Extension of the combination parameter

Lemma 2.1 states that the combined hybrid scheme (2.5)–(2.6) admits a unique convergent solution for $\alpha \in (0,1)$. In what follows we will show that this is also true for $\alpha \in (-\infty, 0) \bigcup (0,1)$.

First we introduce the following definition as in [19]:

Definition 3.1. A weakly compatible finite element space U^h is referred to as completely energy-compatible (or E-compatible) with respect to the moment space $\mathbf{V}^h$ if

$$b_1(\tau, v - T_c(v)) = 0, \quad \forall(\tau, v) \in \mathbf{V}^h \times U^h. \tag{3.1}$$

Based on this E-compatibility condition, the problem (2.5)–(2.6) reduces to:

Find $(\sigma_h, u_h) \in \mathbf{V}^h \times U^h$, such that

$$\alpha a(\sigma_h, \tau) - \alpha b_2(\tau, u_h) = 0 \quad \forall \tau \in \mathbf{V}^h, \tag{3.2}$$

$$\alpha b_2(\sigma_h, v) + (1-\alpha) d(u_h, v) = f(v) \quad \forall v \in U^h. \tag{3.3}$$

Since $a(\mathbf{m}(\mathbf{D}_2 u_h), \tau) = b_2(\tau, u_h)$ and $a(\mathbf{m}(\mathbf{D}_2 u_h), \mathbf{m}(\mathbf{D}_2 v)) = d(u_h, v)$, for $\alpha \neq 0$ the Eqs. (3.2) and (3.3) can be rewritten in the form

$$a(\sigma_h, \tau) - b_2(\tau, u_h) + b_2(\sigma_h, v) + (1-\alpha) a(\sigma_h - \mathbf{m}(\mathbf{D}_2 u_h), \tau - \mathbf{m}(\mathbf{D}_2 v)) = f(v) \tag{3.4}$$

for $\forall(\tau, v) \in \mathbf{V}^h \times U^h$. This can be viewed as a Galerkin/least-squares stabilized finite element scheme, where the term $(1-\alpha) a(\sigma_h - \mathbf{m}(\mathbf{D}_2 u_h), \tau - \mathbf{m}(\mathbf{D}_2 v))$ is the imposed stabilization term for the scheme

$$a(\sigma_h, \tau) - b_2(\tau, u_h) + b_2(\sigma_h, v) = f(v), \quad \forall(\tau, v) \in \mathbf{V}^h \times U^h.$$

When $1-\alpha>0$, from $a(\tau,\tau)+(1-\alpha)a(\tau-\mathbf{m}(\mathbf{D}_2v),\tau-\mathbf{m}(\mathbf{D}_2v))=0$ we have $\tau=0$ and $v=0$ for the weakly compatible space U^h (see Definition 2.1). So

$$[a(\tau,\tau)+(1-\alpha)a(\tau-\mathbf{m}(\mathbf{D}_2v),\tau-\mathbf{m}(\mathbf{D}_2v))]^{\frac{1}{2}}$$

is a norm of $\mathbf{V}^h\times U^h$. From the equivalence of any two norms in a finite-dimensional space we immediately get

$$a(\tau,\tau)+(1-\alpha)a(\tau-\mathbf{m}(\mathbf{D}_2v),\tau-\mathbf{m}(\mathbf{D}_2v))\geqslant C\left(\|\tau\|_{\mathbf{V}}^2+\|v\|_U^2\right). \tag{3.5}$$

According to the Lax–Milgram theorem, the existence and uniqueness of the discrete solution of the scheme (3.4) follow naturally. Furthermore, we have

Theorem 3.1. *Let $(\sigma,u)\in H(\mathbf{divdiv},\Omega)\times H_0^2(\Omega)$ be the exact solution to problem (2.1). Assume that U^h is weakly compatible and E-compatible with respect to $\mathbf{V}^h$ with*

$$|b_1(\tau,v-T_c(v))|\leqslant C\|\tau\|_{\mathbf{V}}\|v\|_U,\quad \forall(\tau,v)\in\mathbf{V}\times U^h. \tag{3.6}$$

Then, for any $\alpha\in(-\infty,0)\bigcup(0,1)$, the problem (3.4) admits a unique solution $(\sigma_h,u_h)\in\mathbf{V}^h\times U^h$ such that the following error estimate holds:

$$\|\sigma-\sigma_h\|_{0,\Omega}+\|u-u_h\|_U\leqslant C\left\{\inf_{\tau\in\mathbf{V}^h}\|\sigma-\tau\|_{\mathbf{V}}+\inf_{v\in U^h}\|u-v\|_U\right\}. \tag{3.7}$$

Proof. We only need to prove the estimate (3.7). From the Eqs. (2.3)–(2.4) and $u-u_c=0$, $\nabla(u-u_c)\cdot\mathbf{n}=0$ on $\partial\Omega$, the exact solution (σ,u) of the problem (2.1) satisfies, for $(\tau,v)\in\mathbf{V}^h\times U^h$,

$$a(\sigma,\tau)-b_2(\tau,u)+b_2(\sigma,v)-b_1(\sigma,v-T_c(v))+(1-\alpha)a(\sigma-\mathbf{m}(\mathbf{D}_2u),\tau-\mathbf{m}(\mathbf{D}_2v))=f(v). \tag{3.8}$$

Let $(I_1\sigma,I_0u)\in\mathbf{V}^h\times U^h$ be any given approximation of (σ,u). Subtracting (3.4) from (3.8), we have

$$\begin{aligned}&a(I_1\sigma-\sigma_h,\tau)-b_2(\tau,I_0u-u_h)+b_2(I_1\sigma-\sigma_h,v)+(1-\alpha)a(I_1\sigma-\sigma_h-\mathbf{m}(\mathbf{D}_2(I_0u-u_h)),\tau-\mathbf{m}(\mathbf{D}_2v))\\&\quad=a(I_1\sigma-\sigma,\tau)-b_2(\tau,I_0u-u)+b_2(I_1\sigma-\sigma,v)-b_1(I_1\sigma-\sigma,v-T_c(v))\\&\qquad+(1-\alpha)a(I_1\sigma-\sigma-\mathbf{m}(\mathbf{D}_2(I_0u-u)),\tau-\mathbf{m}(\mathbf{D}_2v)).\end{aligned}$$

Taking $\tau=I_1\sigma-\sigma_h=:\delta\sigma_h$, $v=I_0u-u_h=:\delta u_h$ in the above equation, we get

$$\begin{aligned}&a(\delta\sigma_h,\delta\sigma_h)+(1-\alpha)a(\delta\sigma_h-\mathbf{m}(\mathbf{D}_2\delta u_h),\delta\sigma_h-\mathbf{m}(\mathbf{D}_2\delta u_h))\\&\quad=a(I_1\sigma-\sigma,\delta\sigma_h)-b_2(\delta\sigma_h,I_0u-u)+b_2(I_1\sigma-\sigma,\delta u_h)-b_1(I_1\sigma-\sigma,\delta u_h-T_c(\delta u_h))\\&\qquad+(1-\alpha)a(I_1\sigma-\sigma-\mathbf{m}(\mathbf{D}_2(I_0u-u)),\delta\sigma_h-\mathbf{m}(\mathbf{D}_2\delta u_h))\\&\quad=(2-\alpha)a(I_1\sigma-\sigma,\delta\sigma_h)-(2-\alpha)b_2(\delta\sigma_h,I_0u-u)+\alpha b_2(I_1\sigma-\sigma,\delta u_h)\\&\qquad+(1-\alpha)d(I_0u-u,\delta u_h)-b_1(I_1\sigma-\sigma,\delta u_h-T_c(\delta u_h))=:\sum(\sigma,u).\end{aligned}$$

By virtue of the Schwartz inequality and $|b_2(\tau,v)|\leqslant a^{1/2}(\tau,\tau)\cdot d^{1/2}(v,v)$, and by (3.6), we have

$$\begin{aligned}\sum(\sigma,u)&\leqslant(2-\alpha)a^{\frac{1}{2}}(I_1\sigma-\sigma,I_1\sigma-\sigma)\cdot a^{\frac{1}{2}}(\delta\sigma_h,\delta\sigma_h)+(2-\alpha)a^{\frac{1}{2}}(\delta\sigma_h,\delta\sigma_h)\cdot d^{\frac{1}{2}}(I_0u-u,I_0u-u)\\&\quad+\alpha a^{\frac{1}{2}}(I_1\sigma-\sigma,I_1\sigma-\sigma)\cdot d^{\frac{1}{2}}(\delta u_h,\delta u_h)+(1-\alpha)d^{\frac{1}{2}}(I_0u-u,I_0u-u)\cdot d^{\frac{1}{2}}(\delta u_h,\delta u_h)+C\|I_1\sigma-\sigma\|_{\mathbf{V}}\|\delta u_h\|_U\\&\leqslant C\Big\{a^{\frac{1}{2}}(\delta\sigma_h,\delta\sigma_h)\Big[a^{\frac{1}{2}}(I_1\sigma-\sigma,I_1\sigma-\sigma)+d^{\frac{1}{2}}(I_0u-u,I_0u-u)\Big]\\&\quad+d^{\frac{1}{2}}(\delta u_h,\delta u_h)\Big[a^{\frac{1}{2}}(I_1\sigma-\sigma,I_1\sigma-\sigma)+d^{\frac{1}{2}}(I_0u-u,I_0u-u)\Big]+\|I_1\sigma-\sigma\|_{\mathbf{V}}\|\delta u_h\|_U\Big\}\\&\leqslant C\Big\{[a(\delta\sigma_h,\delta\sigma_h)+d(\delta u_h,\delta u_h)]^{\frac{1}{2}}\cdot[a(I_1\sigma-\sigma,I_1\sigma-\sigma)+d(I_0u-u,I_0u-u)]^{\frac{1}{2}}+\|I_1\sigma-\sigma\|_{\mathbf{V}}\|\delta u_h\|_U\Big\}.\end{aligned}$$

Since

$$\begin{aligned}&\|v\|_U\leqslant Cd^{\frac{1}{2}}(v,v)\leqslant C\|v\|_U,\quad a^{\frac{1}{2}}(\tau,\tau)\leqslant C\|\tau\|_{\mathbf{V}},\\&d(v,v)\leqslant C\{a(\tau,\tau)+a(\tau-\mathbf{m}(\mathbf{D}_2v),\tau-\mathbf{m}(\mathbf{D}_2v))\},\end{aligned}$$

using Schwartz inequality, we further have

$$\begin{aligned}\sum(\sigma,u)&\leqslant C[a(\delta\sigma_h,\delta\sigma_h)+d(\delta u_h,\delta u_h)]^{\frac{1}{2}}\cdot[a(I_1\sigma-\sigma,I_1\sigma-\sigma)+d(I_0u-u,I_0u-u)+\|I_1\sigma-\sigma\|_{\mathbf{V}}^2]^{\frac{1}{2}}\\&\leqslant C[a(\delta\sigma_h,\delta\sigma_h)+a(\delta\sigma_h-\mathbf{m}(\mathbf{D}_2\delta u_h),\delta\sigma_h-\mathbf{m}(\mathbf{D}_2\delta u_h))]^{\frac{1}{2}}\cdot\left[\|\sigma-I_1\sigma\|_{\mathbf{V}}^2+\|u-I_0u\|_U^2\right]^{\frac{1}{2}}.\end{aligned}$$

Hence, by the definition of $\sum(\sigma,u)$, we get

$$a(\delta\sigma_h,\delta\sigma_h)+a(\delta\sigma_h-\mathbf{m}(\mathbf{D}_2\delta u_h),\delta\sigma_h-\mathbf{m}(\mathbf{D}_2\delta u_h))\leqslant C\Big\{\|\sigma-I_1\sigma\|^2_{\mathbf{V}}+\|u-I_0u\|^2_U\Big\}.$$

Therefore,

$$\|\delta\sigma_h\|_{0,\Omega}+\|\delta u_h\|_U\leqslant C\{\|\sigma-I_1\sigma\|_{\mathbf{V}}+\|u-I_0u\|_U\}.$$

Finally, by triangular inequality and arbitrariness of $(I_1\sigma, I_0u)$, we obtain the desired estimate (3.7). □

Notice that in this theorem the admissible interval of the combination parameter α becomes $(-\infty,0)\bigcup(0,1)$, while in Lemma 2.1 it is $(0,1)$. In what follows, we shall discuss the advantage of this extension of α in the energy adjustment of the discretized model.

3.2. Energy adjustment by the combination parameter

The saddle-point form of the problem (3.2)–(3.3) reads as:

$$\Pi_{CH}(\sigma_h,u_h;\alpha)=\inf_{v\in U^h}\sup_{\tau\in\mathbf{V}^h}\Pi_{CH}(\tau,v;\alpha),$$

where the energy functional

$$\Pi_{CH}(\tau,v;\alpha):=\frac{1-\alpha}{2}d(v,v)-f(v)+\alpha\Big[b_2(\tau,v)-\frac{1}{2}a(\tau,\tau)\Big].$$

We can rewrite the above saddle-point form as

$$\begin{aligned}\Pi_{CH}(\sigma_h,u_h;\alpha)&=\inf_{v\in U^h}\sup_{\tau\in\mathbf{V}^h}\Big\{\frac{1-\alpha}{2}d(v,v)-f(v)+\alpha\Big[b_2(\tau,v)-\frac{1}{2}a(\tau,\tau)\Big]\Big\}\\&=\inf_{v\in U^h}\Big\{\frac{1}{2}d(v,v)-f(v)+\sup_{\tau\in\mathbf{V}^h}\alpha\Big[-\frac{1}{2}a(\tau,\tau)+b_2(\tau,v)-\frac{1}{2}d(v,v)\Big]\Big\}\\&=\inf_{v\in U^h}\Big\{\frac{1}{2}d(v,v)-f(v)+\sup_{\tau\in\mathbf{V}^h}\frac{-\alpha}{2}a(\tau-\mathbf{m}(\mathbf{D}_2v),\tau-\mathbf{m}(\mathbf{D}_2v))\Big\}.\end{aligned}$$

From this novel formulation, we have the following conclusion:

Proposition 3.1. *For given spaces U^h and $\mathbf{V}^h$ with $\mathbf{V}^h\not\supseteq\mathbf{m}(\mathbf{D}_2U^h)$, the energy functional $\Pi_{CH}(\sigma_h,u_h;\alpha)$ depends on α continuously, and $\Pi_{CH}(\sigma_h,u_h;\alpha)$ is monotone decreasing with respect to $\alpha\in(-\infty,0)\bigcup(0,1)$, i.e. for $\alpha_1,\alpha_2\in(-\infty,0)\bigcup(0,1)$, $\alpha_1<\alpha_2$ implies*

$$\Pi_{CH}(\sigma_h,u_h;\alpha_1)\geqslant\Pi_{CH}(\sigma_h,u_h;\alpha_2).$$

Moreover, there holds $\lim_{\alpha\to-\infty}\Pi_{CH}(\sigma_h,u_h;\alpha)=+\infty$.

Proposition 3.1 clarifies the energy-adjusting mechanism of the CHFE method and the role of the combination parameter α in adjusting the energy of the discretized model. As shown in [20–22], higher energy-accuracy schemes generally enjoy higher numerical accuracy. Then, in this sense, the CHFE method can improve the given displacement model

$$\Pi_P(u_1^h)=\inf_{v\in U^h}\Pi_P(v)$$

by adjusting the combination parameter α such that the energy-error inequality

$$|\Pi_{CH}(\sigma_h,u_h;\alpha)-\Pi_P(u)|<|\Pi_P(u_1^h)-\Pi_P(u)| \tag{3.9}$$

holds, where $\Pi_P(v)=\Pi_{CH}(\tau,v;0)=\frac{1}{2}d(v,v)-f(v)$ denotes the potential energy functional and $\Pi_P(u)=\inf_{v\in H_0^2(\Omega)}\Pi_P(v)$ is the exact energy. In other words, an appropriate choice of α can lead to a CHFE scheme with energy-accuracy more accurate than the corresponding displacement scheme.

For the weakly compatible subspace U^h, we consider the following two cases:

Case 1. The potential energy $\Pi_P(u_1^h)$ satisfies

$$\Pi_P(u_1^h)>\Pi_P(u); \tag{3.10}$$

Case 2. There holds

$$\Pi_P(u_1^h)<\Pi_P(u). \tag{3.11}$$

For Case 1, according to Proposition 3.1, for a given bending moment subspace $\mathbf{V}^h$, we can realize the improvement (3.9) by adjusting the parameter $\alpha \in (0,1)$, whereas for Case 2, we can obtain (3.9) by adjusting the parameter $\alpha \in (-\infty, 0)$.

Especially, for Case 2, from Proposition 3.1,there exists $\bar{\alpha} \in (-\infty, 0)$ such that

$$\Pi_{CH}(\sigma_h, u_h; 0) = \Pi_P(u_1^h) < \Pi_P(u) < \Pi_{CH}(\sigma_h, u_h; \bar{\alpha}). \tag{3.12}$$

Thus, by the continuity of the energy functional $\Pi_{CH}(\sigma_h, u_h; \alpha)$ with respect to α, we easily know that there exists a parameter $\alpha^* \in (-\infty, 0)$ such that the combined hybrid scheme (3.2)–(3.3) is of zero energy-error, i.e. there holds the energy relation

$$\Pi_{CH}(\sigma_h, u_h; \alpha^*) = \Pi_P(u). \tag{3.13}$$

Remark 3.1. Theoretically the optimal choice α^* in (3.13) can be approximately found out by a bisection algorithm. In fact, assume that for an appropriately coarse mesh with mesh size h and its finer mesh with size $h/2$, the energy $\Pi_{CH}(\sigma_h, u_h; \alpha)$ at fine mesh is more accurate than at the coarse mesh. Then different accuracy-altered trends at two ends of interval $(\bar{\alpha}, 0)$ will occur, where $\bar{\alpha}$ is the same as in (3.12). At $\alpha = 0$, the energy increases in the direction from h to $h/2$, while it decreases at $\alpha = \bar{\alpha}$. Utilizing this difference in trend, the altered trend at $\alpha' = \bar{\alpha}/2$ can be used to decide the optimal α^* being inside which one of two intervals $(\bar{\alpha}, \alpha')$ and $(\alpha', 0)$, and a better $\bar{\alpha}^*$ than α' can be determined.

4. Application: improvement of Adini's rectangular element

As an application of the above theory for the parameter extension, this section is devoted to improvement of Adini's rectangular element by the CHFE method.

Assume that Ω is a rectangular domain and $\Omega_i \in T_h$ is an arbitrary rectangle with vertices $Q_j(x_j, y_j)$, $j = 1, 2, 3, 4$, central point (x_0, y_0), and side lengthes h_x and h_y.

The deflection subspace of Adini's C^0-interpolants is defined as [5]

$$U_A^h = \left\{ v \in U \bigcap C^0(\bar{\Omega});\ v_{|\Omega_i} \in P_3(\Omega_i) \oplus \bigvee \{xy^3, x^3y\},\ \ \forall \Omega_i \in T_h \right\},$$

with the set of nodal parameters on Ω_i

$$\Pi_{\Omega_i} = \{v(Q_j), \partial_1 v(Q_j), \partial_2 v(Q_j), \quad j = 1, 2, 3, 4\}.$$

Let $\widehat{\Omega}_i = [-1, 1]^2$ be the referential square with four vertices

$$\widehat{Q}_1 = (\xi_1, \eta_1) = (-1, -1), \quad \widehat{Q}_2 = (\xi_2, \eta_2) = (1, -1),$$
$$\widehat{Q}_3 = (\xi_3, \eta_3) = (1, 1), \quad \widehat{Q}_4 = (\xi_4, \eta_4) = (-1, 1).$$

The local co-ordinates ξ and η on $\widehat{\Omega}_i$ are given by

$$\xi = 2(x - x_0)/h_x, \quad \eta = 2(y - y_0)/h_y.$$

Then for $\forall \hat{v} \in P_3(\widehat{\Omega}_i) \oplus \bigvee \{\xi\eta^3, \xi^3\eta\}$, we can write

$$\hat{v} = \sum_{j=1}^{4} \left(\hat{v}(j) p_j + \hat{v}_\xi(j) \phi_j + \hat{v}_\eta(j) \psi_j \right),$$

with

$$\begin{cases} p_j = \frac{(1+\xi_j\xi)(1+\eta_j\eta)}{4} \left(1 + \frac{\xi_j\xi + \eta_j\eta}{2} - \frac{\xi^2 + \eta^2}{2}\right), \\ \phi_j = -\frac{(1+\eta_j\eta)(1+\xi_j\xi)^2(1-\xi_j\xi)}{8} \xi_j, \\ \psi_j = -\frac{(1+\xi_j\xi)(1+\eta_j\eta)^2(1-\eta_j\eta)}{8} \eta_j, \end{cases}$$

where $\hat{v}(j), \hat{v}_\xi(j), \hat{v}_\eta(j)$ $(j = 1, 2, 3, 4)$ denote the twelve degrees of freedom on $\widehat{\Omega}_i$.

Consider the following two kinds of bending moment modes [21]: the piecewise-constant mode $\mathbf{V}_0^h$ and the piecewise-incomplete-quadratic mode $\mathbf{V}_{0-2}^h$. They are defined, respectively, as

$$\forall \tau \in \mathbf{V}_0^h, \tau_{|\Omega_i} = \begin{pmatrix} \tau_{11} \\ \tau_{22} \\ \tau_{12} \end{pmatrix} = \begin{pmatrix} 1 & 0 & 0 \\ 0 & 1 & 0 \\ 0 & 0 & 1 \end{pmatrix} \begin{pmatrix} \beta_1 \\ \beta_2 \\ \beta_3 \end{pmatrix}, \tag{4.1}$$

$$\forall \tau \in \mathbf{V}_{0-2}^h, \tau_{|\Omega_i} = \begin{pmatrix} \tau_{11} \\ \tau_{22} \\ \tau_{12} \end{pmatrix} = \begin{pmatrix} 1 & 0 & 0 & \eta & 0 & 0 & 0 & \xi^2 & 0 & 0 & \eta^2 & 0 & 0 \\ 0 & 1 & 0 & 0 & \xi & 0 & 0 & 0 & \xi^2 & 0 & 0 & \eta^2 & 0 \\ 0 & 0 & 1 & 0 & 0 & \xi & \eta & 0 & 0 & \xi^2 & 0 & 0 & \eta^2 \end{pmatrix} \begin{pmatrix} \beta_1 \\ \vdots \\ \beta_{13} \end{pmatrix}. \tag{4.2}$$

Since $U_A^h \subset C^0(\overline{\Omega})$, from Remark 2.1 we have

$$b_1(\tau, v - T_c(v)) = \sum \oint_{\partial\Omega_i} M_{nn}(\tau)\nabla(v - T_c(v)) \cdot \mathbf{n}\, ds \quad \forall(\tau, v) \in \mathbf{V}^h \times U_A^h.$$

Furthermore, as proved in [21], the E-compatibility condition

$$b_1(\tau, v - T_c(v)) = 0 \quad \forall(\tau, v) \in \mathbf{V}^h \times U_A^h \tag{4.3}$$

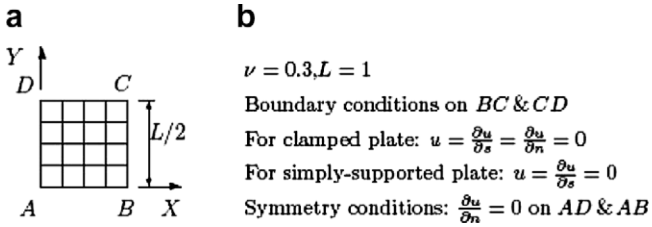

Fig. 1. Quadrant of a square plate: geometry and 4 × 4 mesh.

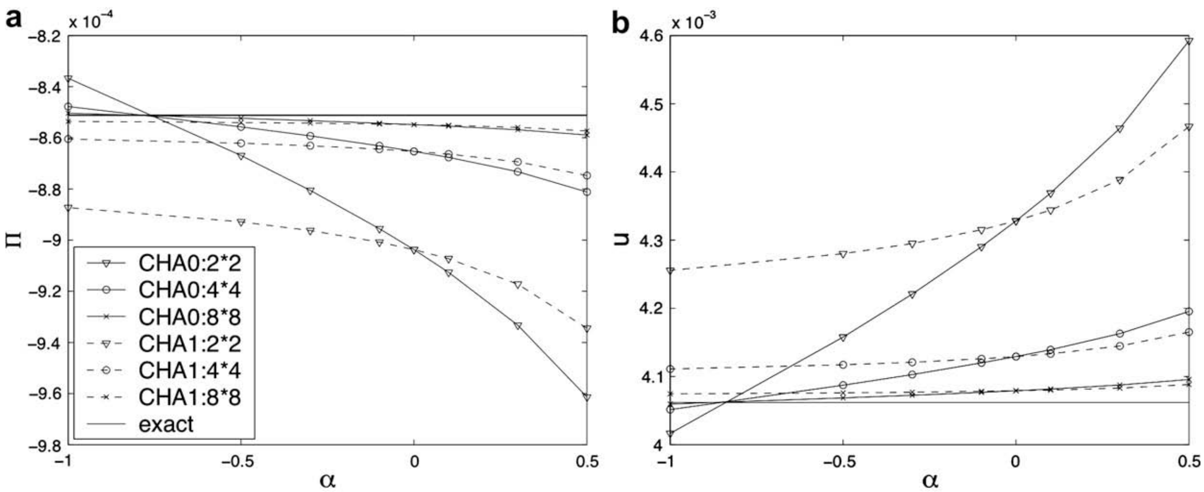

Fig. 2. Energy Π and central displacement u for CHA0 and CHA1: simply-supported boundary and unit uniform load.

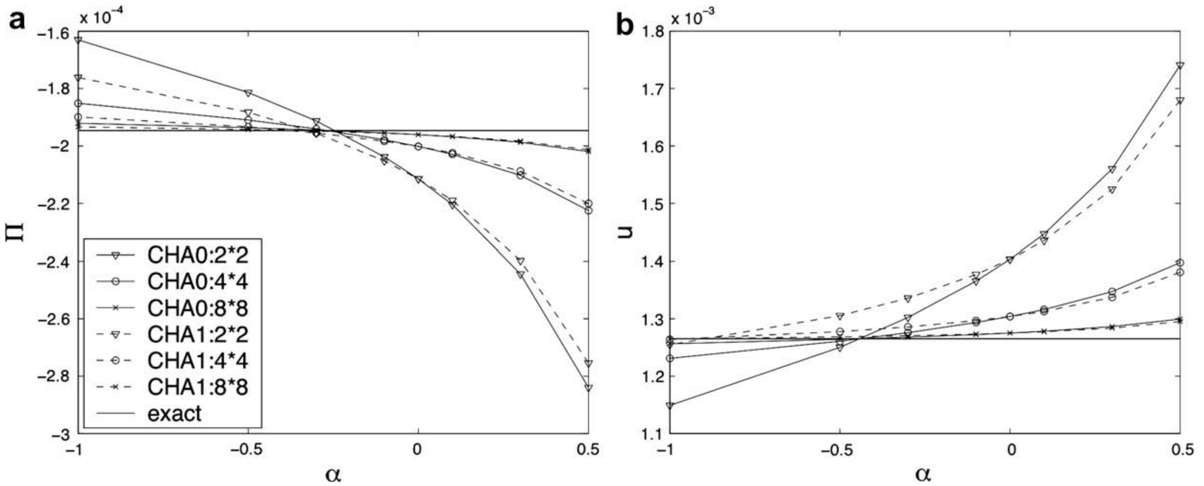

Fig. 3. Energy Π and central displacement u for CHA0 and CHA1: clamped boundary and unit uniform load.

holds, where $\mathbf{V}^h = \mathbf{V}_0^h$ or $\mathbf{V}_{0-2}^h$. We can also easily verify the inequality (3.6) for U_A^h.

Now take $U^h = U_A^h$ in the combined hybrid scheme (3.2)–(3.3), and take $\mathbf{V}^h = \mathbf{V}_0^h$ and $\mathbf{V}^h = \mathbf{V}_{0-2}^h$, respectively, we then obtain the combined hybrid plate elements $\mathbf{V}_0^h \times U_A^h$ and $\mathbf{V}_{0-2}^h \times U_A^h$ which are denoted respectively by CHA0(α) and CHA1(α) [21].

According to Theorem 3.1, the parameter extension is valid for CHA0(α) and CHA1(α), i.e. we can take $\alpha \in (-\infty, 0) \bigcup (0, 1)$.

5. Numerical experiments

Several test problems are calculated with the combined hybrid scheme (3.2)–(3.3) for the combined hybrid elements CHA0(α) and CHA1(α) to show the role of the combination parameter α in reducing the energy error of the discretized model so as to yield accurate displacement results at coarse meshes.

A thin isotropic square plate of side length $L = 1$ and Poisson's ratio $\nu = 0.3$ is considered with two types of boundary conditions (Fig. 1): simply-supported boundary conditions and clamped boundary conditions. The applied transverse loading is in the form of a unit uniform load or a unit center concentrated load.

Table 1
Energy and displacement results: simply-supported boundary and unit center concentrated load.

Element	α	CHA0			CHA1		
		2×2	4×4	8×8	2×2	4×4	8×8
$\Pi(e-3)$	0.5	−6.957	−6.176	−5.916	−6.757	−6.116	−5.898
	0.3	−6.544	−6.038	−5.873	−6.430	−6.004	−5.863
	0.1	−6.272	−5.949	−5.845	−6.235	−5.938	−5.842
	Adini ($\alpha = 0$)	−6.166	−5.914	−5.835	−6.166	−5.914	−5.835
	−0.1	−6.068	−5.884	−5.825	−6.104	−5.895	−5.829
	−0.3	−5.905	−5.831	−5.809	−6.011	−5.864	−5.819
	−0.5	−5.767	−5.788	−5.796	−5.941	−5.841	−5.812
	−1	−5.489	−5.699	−5.769	−5.823	−5.803	−5.800
$u(e-2)$	0.5	1.391	1.235	1.183	1.352	1.223	1.180
	0.3	1.309	1.208	1.175	1.286	1.201	1.173
	0.1	1.254	1190	1.169	1.247	1.188	1.168
	Adini ($\alpha = 0$)	1.233	1.183	1.167	1.233	1.183	1.167
	−0.1	1.214	1.177	1.165	1.221	1.179	1.166
	−0.3	1.181	1.166	1.162	1.202	1.173	1.164
	−0.5	1.153	1.158	1.159	1.188	1.168	1.162
	−1	1.098	1.140	1.154	1.165	1.161	1.160
		12-parameter [25]			BFS [5]		
		1.136	1.155	1.159	1.147	1.157	1.159

Note: Exact $\Pi = -5.801e-3$, $u = 1.160e-2$.

Table 2
Energy and displacement results: clamped boundary and unit center concentrated load.

Element	α	CHA0			CHA1		
		2×2	4×4	8×8	2×2	4×4	8×8
$\Pi(e-3)$	0.5	−3.944	−3.192	−2.925	−3.789	−3.141	−2.910
	0.3	−3.475	−3.036	−2.877	−3.390	−3.007	−2.868
	0.1	−3.180	−2.939	−2.848	−3.153	−2.929	−2.845
	Adini ($\alpha = 0$)	−3.067	−2.901	−2.836	−3.067	−2.901	−2.836
	−0.1	−2.970	−2.869	−2.826	−2.996	−2.878	−2.829
	−0.3	−2.809	−2.815	−2.810	−2.883	−2.842	−2.818
	−0.5	−2.678	−2.770	−2.796	−2.799	−2.815	−2.810
	−1	−2.430	−2.683	−2.769	−2.656	−2.769	−2.797
$u\ (e-3)$	0.5	7.888	6.384	5.851	7.578	6.283	5.819
	0.3	6.950	6.073	5.755	6.780	6.014	5.737
	0.1	6.360	5.877	5.695	6.306	5.859	5.689
	Adini ($\alpha = 0$)	6.135	5.803	5.672	6.135	5.803	5.672
	−0.1	5.940	5.738	5.652	5.992	5.756	5.658
	−0.3	5.617	5.629	5.619	5.766	5.684	5.636
	−0.5	5.356	5.540	5.592	5.597	5.629	5.620
	−1	4.861	5.366	5.538	5.313	5.539	5.593
		12-parameter [25]			BFS [5]		
		5.324	5.544	5.597	5.622	5.597	5.606

Note: Exact $\Pi = -2.806e-3$, $u = 5.612e-3$.

In the elements CHA0(α) and CHA1(α), the combination parameter α is taken respectively as $\alpha = 0.5, 0.3, 0.1, 0, -0.1, -0.3, -0.5, -1$. When $\alpha = 0$, CHA0(0) and CHA1(0) are identical to Adini's element. Three kinds of meshes, (2×2), (4×4) and (8×8), are used. In Figs. 2 and 3, we give graphically the results of the energy Π and the central displacement u for the square plates under simply-supported/clamped boundary conditions and a unit uniform load, whereas in Tables 1 and 2, we list the computational results of the energy and displacement under a unit center concentrated load. From Figs. 2, 3 and Tables 1, 2, we can see that in all the cases, it holds the relation $\Pi_{CH}(\sigma_h, u_h; 0) < \Pi_P(u)$, i.e. Adini's rectangular element satisfies (3.11). Especially, for $\alpha \in (-1, 0)$, the energy results are more accurate than those of Adini's element, and so are the displacement results. We can also see that high accuracy for displacement, as well as for energy, are attained at coarse meshes for appropriate choice of α, say $\alpha = -0.5$ for CHA0(α). Comparisons are made with the conforming Bogner-Fox-Schmit (BFS) element with 16 parameters [5] and the 12-parameter rectangular element proposed by Shi and Chen [25].

6. Conclusions

Equivalence of the combined hybrid finite element scheme and some Galerkin/least-squares stabilized scheme has been established. This extends the choice of the combination parameter α from the interval $(0, 1)$ to $(-\infty, 0) \bigcup (0, 1)$. It has been shown by numerical experiments that high numerical accuracy of the CHFE method can be attained at coarse meshes by appropriately choosing $\alpha \in (-\infty, 0)$.

References

[1] T.-X. Zhou, Finite element method based on combination of 'saddle point' variational formulations, Sci. China (Ser. E) 40 (1997) 285–300.
[2] T.-X. Zhou, Y.-F. Nie, Combined hybrid approach to finite element schemes of high performance, Int. J. Numer. Meth. Eng. 51 (2001) 182–202.
[3] T.-X. Zhou, Stabilized hybrid finite element methods based on combination of saddle point principles of elasticity problem, Math. Comput. 72 (2003) 1655–1673.
[4] F. Brezzi, L.D. Marini, On the numerical solution of plate bending problems by hybrid methods, RAIRO, R-3 9 (1975) 5–50.
[5] P.G. Ciarlet, The Finite Element Method for Elliptic Problems, North-Holland, Amsterdam, 1978.
[6] F. Brezzi, M. Fortin, Mixed and Hybrid Finite Element Methods, Springer, Berlin, 1991.
[7] I. Babuska, The finite element method with penalty, Math. Comput. 27 (1973) 221–228.
[8] I. Babuska, M. Zlamal, Nonconforming elements in the finite element method with penalty, SIAM J. Numer. Anal. 10 (1973) 863–875.
[9] G.F. Carey, A. Kabaila, M. Utku, On penalty methods for interelement constraints, Comput. Meth. Appl. Mech. Eng. 30 (1982) 151–171.
[10] D.N. Arnold, An interior penalty finite element method with discontinuous elements, SIAM J. Numer. Anal. 19 (1982) 742–760.
[11] M. Utku, G.F. Carey, Boundary penalty techniques, Comput. Meth. Appl. Mech. Eng. 30 (1982) 103–118.
[12] P. Monk, A mixed finite element method for the biharmonic equation, SIAM J. Numer. Anal. 24 (1987) 737–749.
[13] O.C. Zienkiewicz, R.L. Taylor, P. Papadopoulos, E. Oñate, Plate bending elements with discrete constraints: new triangular elements, Comput. Struct. 35 (1990) 505–522.
[14] S.L. Weissman, R.L. Taylor, Mixed formulations for plate bending elements, Comput. Meth. Appl. Mech. Eng. 94 (1992) 391–427.
[15] B.N. Jiang, The least-squares finite element method for elasticity. Part II: bending of thin plates, Int. J. Numer. Meth. Eng. 54 (2002) 1459–1475.
[16] J.P. Pontaza, J.N. Reddy, Mixed plate bending elements based on least-squares formulation, Int. J. Numer. Meth. Eng. 60 (2004) 891–922.
[17] J.N. Reddy, A penalty plate-bending element for the analysis of laminated anisotropic composite plates, Int. J. Numer. Meth. Eng. 15 (2005) 1187–1206.
[18] J.N. Reddy, E.J. Barbero, J.L. Teply, A plate bending element based on a generalized laminate plate theory, Int. J. Numer. Meth. Eng. 28 (2005) 2275–2292.
[19] T.-X. Zhou, X.-P. Xie, A combined hybrid method for plate bending problems, J. Comput. Math. 21 (2003) 347–356.
[20] T.-X. Zhou, X.-P. Xie, Zero energy-error mechanism of the combined hybrid method and improvement of Allman's membrane element with drilling d.o.f.'s, Commun. Numer. Meth. Eng. 20 (2004) 241–250.
[21] X.-P. Xie, From energy improvement to accuracy enhancement: improvement of plate bending elements by the combined hybrid method, J. Comput. Math. 22 (2004) 392–581.
[22] X.-P. Xie, J.-C. Hu, Energy-adjustable mechanism of the combined hybrid method and improvement of Zienkiewicz's plate element, Commun. Numer. Meth. Eng. 21 (2005) 531–544.
[23] T.J.R. Hughes, L.P. Franca, G.M. Hulbert, A new finite element formulation for computational fluid dynamics: VIII. The Galerkin/least-squares method for advective–diffusive equations, Comput. Meth. Appl. Mech. Eng. 73 (1989) 173–189.
[24] L.P. Franca, R. Stenberg, Error analysis of some Galerkin least squares methods for the elasticity equations, SIAM J. Numer. Anal. 28 (1991) 1680–1697.
[25] Z.C. Shi, Q.Y. Chen, A rectangular plate element of high accuracy, Sci. China (Ser. A) 6 (2000) 504–515.